

J/ψ as a function of p_T in small systems:
Run15pp, Run15pAu, Run15pAl and Run143HeAu
(Includes pAu Centrality)

Krista Smith, Tony Frawley, Matt Durham and Sanghoon Lim

Florida State University

September 10, 2018

Contents

| | | |
|----------|--|-----------|
| 1 | J/ψ as function of p_T | 3 |
| 1.1 | Fitting | 3 |
| 1.1.1 | Background Estimation | 3 |
| 1.1.2 | Total Fit Function | 4 |
| 1.1.3 | Comparison with Rapidity Analysis | 5 |
| 1.2 | Systematic Uncertainties in Fit | 6 |
| 1.2.1 | Uncertainty Estimation in Fixed Parameters | 6 |
| 1.3 | Bin Shift Corrections | 8 |
| 1.4 | J/ψ Counts | 8 |
| 1.5 | Invariant Yield | 14 |
| 1.5.1 | Invariant Yield Results | 15 |
| 1.6 | Invariant Cross Section | 15 |
| 1.7 | R_{AA} vs. p_T | 16 |
| 1.7.1 | Run15pAu, Run15pAl and Run14HeAu Results | 16 |
| 1.8 | Example Fits | 18 |
| 1.8.1 | Test fits from Run15pAl | 18 |
| 1.8.2 | Sample Fits Using Fixed Correlated Background Parameters | 20 |
| 1.9 | Systematic Uncertainty | 23 |
| 2 | J/ψ as function of Centrality | 24 |
| 2.1 | Fitting | 24 |
| 2.2 | Fixing the Correlated Background Parameters | 24 |
| 2.3 | Systematic Uncertainty due to Correlated Background | 24 |
| 2.4 | J/ψ Counts | 29 |
| 2.5 | R_{AA} as function of Centrality | 29 |
| 2.5.1 | Run15pAu Results | 29 |

1 J/ψ as function of p_T

1.1 Fitting

The fits were done based on the same fitting code that was used by Matt Durham and Sanghoon Lim for the analysis of J/ψ as a function of rapidity, discussed in Section 4.3 of Analysis Note 1354.

1.1.1 Background Estimation

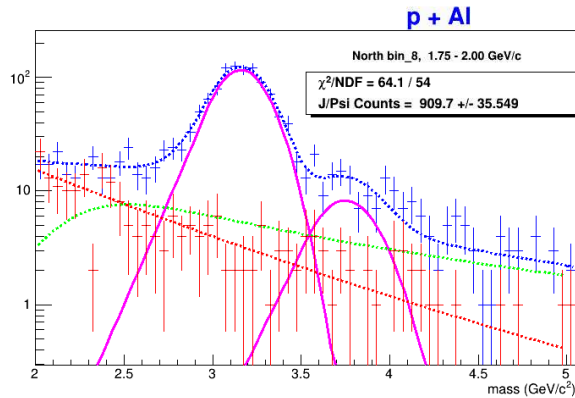
The background consists of correlated and uncorrelated identified "muons". The combinatoric background was estimated by fitting the like-sign muon pairs and normalizing it according to AN 1354 section 4.2. The correlated background was estimated using the following formula, also taken from AN 1354 (Eq. 2):

$$y = \frac{c}{(e^{-ax-bx^2} + x/d)^e}$$

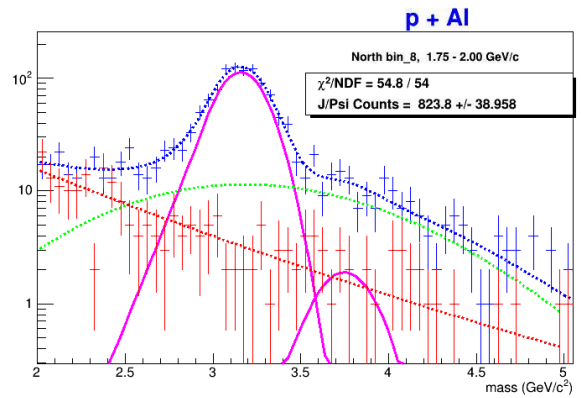
Figure 1: The correlated background formula, which consists of 5 parameters that are all included in the total fit function.

Parameters a, b, c, d, e then become a part of the 13 total fit parameters (see below). Working with this function as an estimation of the correlated background signal, we noticed that the J/ψ counts varied depending on the shape of the correlated background that was chosen, sometimes up to 10% (see figures).

We do not know the shape of the correlated background curve. Therefore, we chose a shape, and used that shape across the entire system. The shape we chose was the one that most closely matched the results reported in AN 1354, as that would imply the same background shape had



(a) Run15pAl North arm example fit with a distinct correlated background shape. p_T range 1.75 - 2.00 GeV/c shown.



(b) For the same North arm p_T range but a different correlated background shape, the J/ψ counts vary by 9.3%.

been selected. To achieve this, we fitted the integrated p_T across each system and selected the set of correlated background parameters that produced a yield that most closely matched the yields reported in AN 1354.

We then applied the same initial starting values for the correlated background parameters as used in the best integrated p_T fit. Then we fixed the pt spectrum to read in these same values. This is discussed in more detail in section 2.2. Therefore, the pt spectrum in each arm was fitted with the same correlated background shape as the p_T integrated. In the case of Run15pp, the north and south arm p_T integrated and p_T spectra were fitted using one set of correlated background starting parameters.

See section 1.8 for examples of fits using the same correlated background starting parameters applied to various p_T ranges for all systems.

1.1.2 Total Fit Function

The total fitting function consists of the sum of a Crystal Ball function for the J/ψ , a separate Crystal Ball function for the ψ' and a correlated background function, as described above.

In the Crystal Ball function, there are five parameters: n , α , N , \bar{x} and σ . The first two are the tail parameters and the remaining three are the Gaussian parameters.

$$f(x; \alpha, n, \bar{x}, \sigma) = N \cdot \begin{cases} \exp\left(-\frac{(x-\bar{x})^2}{2\sigma^2}\right), & \text{for } \frac{x-\bar{x}}{\sigma} > -\alpha \\ A \cdot \left(B - \frac{x-\bar{x}}{\sigma}\right)^{-n}, & \text{for } \frac{x-\bar{x}}{\sigma} \leq -\alpha \end{cases}$$

Figure 3: The Crystal ball function. It is the combination of a Gaussian and power function.

$$A = \left(\frac{n}{|\alpha|}\right)^n \cdot \exp\left(-\frac{|\alpha|^2}{2}\right)$$

$$B = \frac{n}{|\alpha|} - |\alpha|,$$

Figure 4: Expanded parameters A and B for the power function component.

These tail parameters we assume are shared by both the J/ψ and the ψ' , and therefore only one set of tail parameters is needed. This reduces the ten Crystal Ball parameters to eight. Additionally, there are two more ψ' Crystal ball parameters we assume to be known: σ and \bar{x} . The width of the ψ' peak, σ , was set to 1.15 times the width of the J/ψ peak, found through simulations of the muon arm mass resolution as described in section 4.3. And the center of the ψ' peak, \bar{x} , was set to the J/ψ and ψ' mass difference (0.59 GeV/c²).

1.1.3 Comparison with Rapidity Analysis

This analysis is done as an addition to the work done by Matt Durham and Sanghoon Lim, for which AN 1354 describes. The previous analysis included J/ψ as a function of rapidity in the same four small systems we are also analyzing: Run15pp, Run15pAu, Run15pAl and Run143HeAu.

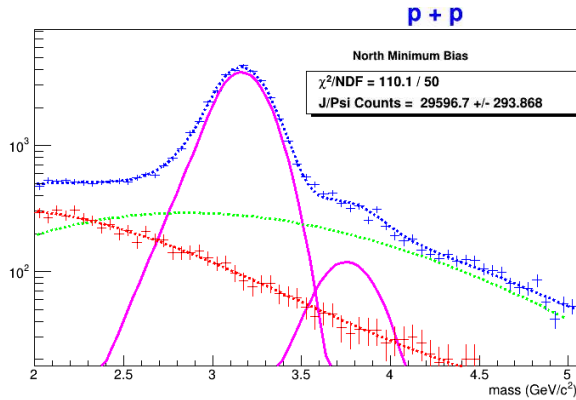
Since we are using the same data sets, and extracting the same J/ψ data as a whole, we checked that the total number of J/ψ counts over the full p_T range for each small system agreed with the total number of J/ψ counts over the full rapidity range (to within 5%). See following figures and Tables 1, 2 for these results.

Table 1: North Arm: Results for p_T integrated raw J/ψ counts compared with results for y integrated raw J/ψ counts (see Section 4.7).

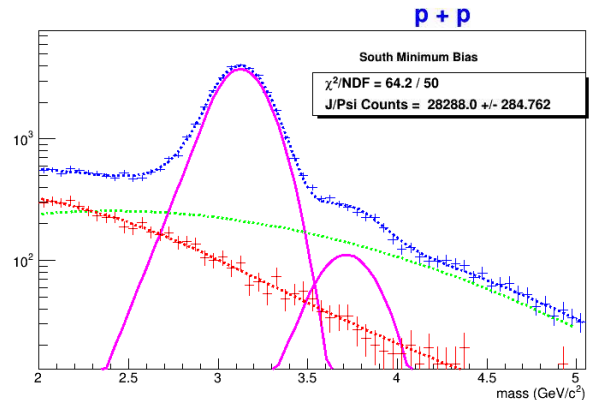
| system | Present Analysis (p_T integrated) | Previous Analysis (y integrated) | % diff |
|------------|---|--|--------|
| Run15 pp | $29,597 \pm 294$ | $29,399 \pm 279$ | +0.67 |
| Run15 pAu | $18,091 \pm 244$ | $18,194 \pm 224$ | -0.57 |
| Run15 pAl | $11,158 \pm 195$ | $11,085 \pm 190$ | +0.66 |
| Run14 HeAu | $3,745 \pm 103$ | $3,825 \pm 91$ | -2.11 |

Table 2: South Arm: Results for p_T integrated raw J/ψ counts compared with results for y integrated raw J/ψ counts (see Section 4.7).

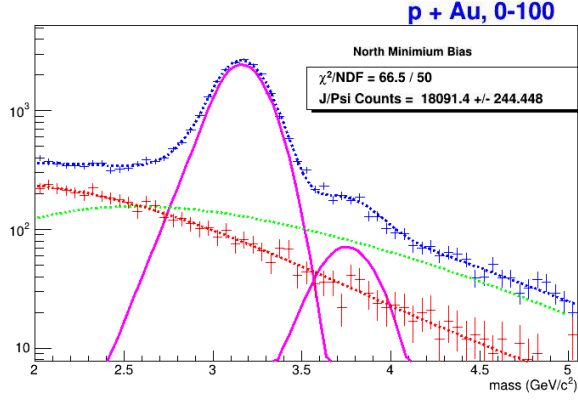
| system | Present Analysis (p_T integrated) | Previous Analysis (y integrated) | % diff |
|------------|---|--|--------|
| Run15 pp | $28,288 \pm 285$ | $28,207 \pm 282$ | +0.29 |
| Run15 pAu | $11,712 \pm 256$ | $11,602 \pm 193$ | +0.94 |
| Run15 pAl | $6,660 \pm 138$ | $6,567 \pm 206$ | +1.41 |
| Run14 HeAu | $4,114 \pm 99$ | $3,987 \pm 118$ | +3.14 |



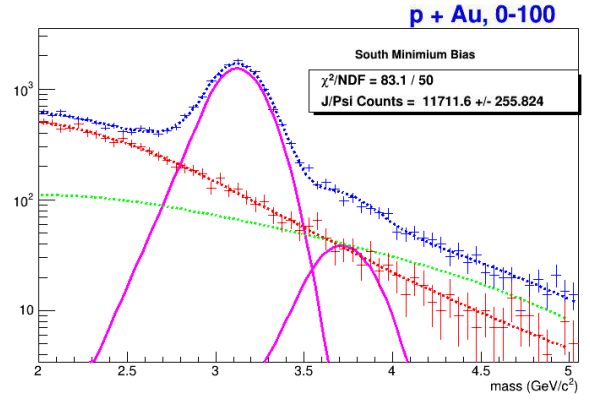
(a) Run15pp p_T integrated, North Arm.



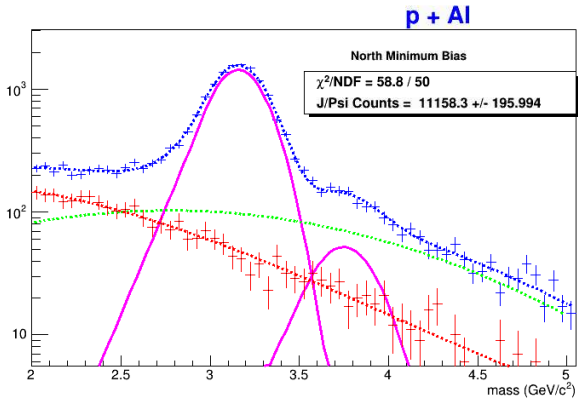
(b) Run15pp p_T integrated, South Arm.



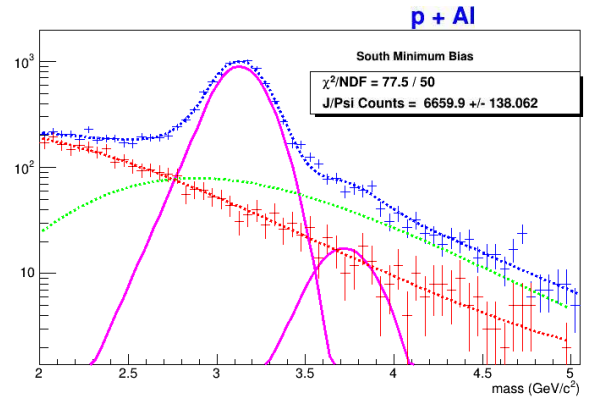
(a) Run15pAu p_T integrated, North Arm.



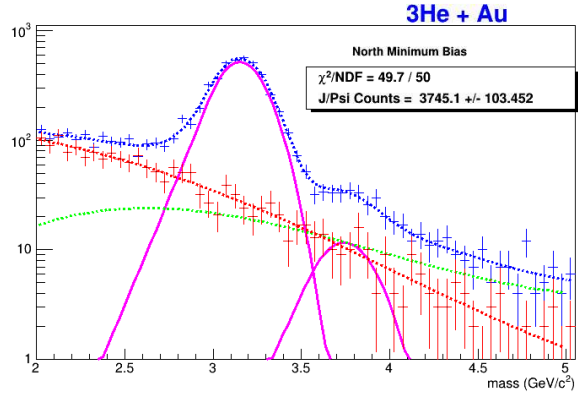
(b) Run15pAu p_T integrated, South Arm.



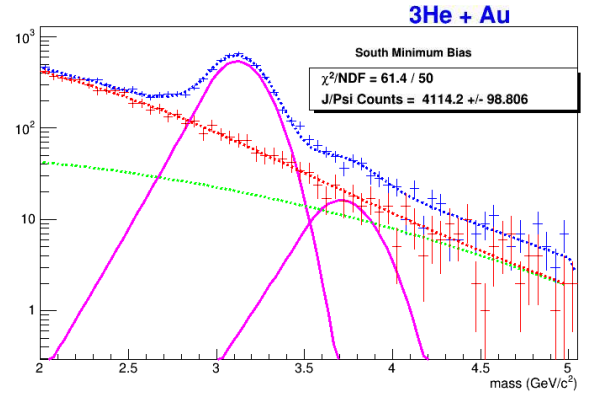
(a) Run15pAl p_T integrated, North Arm.



(b) Run15pAl p_T integrated, South Arm.



(a) Run14HeAu p_T integrated, North Arm.



(b) Run14HeAu p_T integrated, South Arm.

1.2 Systematic Uncertainties in Fit

1.2.1 Uncertainty Estimation in Fixed Parameters

As a result of fixing the correlated background parameters, we calculated the systematic uncertainty arising from this approach (see section 2.3 for details). The results of the study are shown in

the following tables. This systematic uncertainty was included in the overall RAA uncertainty as a Type B uncertainty.

Table 3: Run15pp. Scaled uncertainties for each sampled "test" fit, with the test fit p_T bin and corresponding average for each arm.

| p_T [GeV/c] | Scaled Uncertainty, N | p_T [GeV/c] | Scaled Uncertainty, S |
|--------------------------|-------------------------|--------------------------|-------------------------|
| 0.75 – 1.00 | 0.0339 | 0.50 – 0.75 | 0.0237 |
| 1.50 – 1.75 | 0.0313 | 0.75 – 1.00 | 0.0264 |
| 1.27 – 2.00 | 0.0326 | 1.25 – 1.50 | 0.0242 |
| 2.00 – 2.25 | 0.0385 | 1.50 – 1.75 | 0.0284 |
| 2.50 – 2.75 | 0.0291 | 1.75 – 2.00 | 0.0212 |
| Ave. Uncertainty: | 0.0331 | Ave. Uncertainty: | 0.0248 |

Table 4: Run15pAu. Scaled uncertainties for each sampled "test" fit, with the test fit p_T bin and corresponding average for each arm.

| p_T [GeV/c] | Scaled Uncertainty, N | p_T [GeV/c] | Scaled Uncertainty, S |
|--------------------------|-------------------------|--------------------------|-------------------------|
| 1.25 – 1.50 | 0.0388 | 0.25 – 0.50 | 0.0144 |
| 1.50 – 1.75 | 0.0410 | 1.25 – 1.50 | 0.0184 |
| 2.00 – 2.25 | 0.0303 | 1.50 – 1.75 | 0.0207 |
| 2.25 – 2.50 | 0.0327 | 2.25 – 2.50 | 0.0107 |
| 2.50 – 2.75 | 0.0388 | 2.75 – 3.00 | 0.0173 |
| Ave. Uncertainty: | 0.0363 | Ave. Uncertainty: | 0.0163 |

Table 5: Run15pAl. Scaled uncertainties for each sampled "test" fit, with the test fit p_T bin and corresponding average for each arm.

| p_T [GeV/c] | Scaled Uncertainty, N | p_T [GeV/c] | Scaled Uncertainty, S |
|--------------------------|-------------------------|--------------------------|-------------------------|
| 0.25 – 0.50 | 0.0189 | 0.25 – 0.50 | 0.0310 |
| 1.00 – 1.25 | 0.0325 | 0.50 – 0.75 | 0.0279 |
| 1.50 – 1.75 | 0.0294 | 1.50 – 1.75 | 0.0290 |
| 1.75 – 2.00 | 0.0630 | 1.75 – 2.00 | 0.0302 |
| 2.50 – 2.75 | 0.0355 | 2.50 – 2.75 | 0.0136 |
| Ave. Uncertainty: | 0.0359 | Ave. Uncertainty: | 0.0264 |

Table 6: Run14HeAu. Scaled uncertainties for each sampled "test" fit, with the test fit p_T bin and corresponding average for each arm.

| p_T [GeV/c] | Scaled Uncertainty, N | p_T [GeV/c] | Scaled Uncertainty, S |
|--------------------------|-------------------------|--------------------------|-------------------------|
| 0.50 – 0.75 | 0.0100 | 0.50 – 0.75 | 0.0161 |
| 1.50 – 1.75 | 0.0107 | 1.00 – 1.25 | 0.0128 |
| 1.75 – 2.00 | 0.0241 | 1.25 – 1.50 | 0.0168 |
| 2.00 – 2.25 | 0.0316 | 1.75 – 2.00 | 0.0222 |
| 2.50 – 2.75 | 0.0102 | 2.00 – 2.25 | 0.0060 |
| Ave. Uncertainty: | 0.0173 | Ave. Uncertainty: | 0.0148 |

1.3 Bin Shift Corrections

Bin shift corrections were applied following the method described by Darren McGlinchey, Anthony Frawley and Cesar Luiz da Silva in section 1 of Analysis Note 1001.

There are two bin shift corrections methods presented in the note. Here, we have used the method in which the data point is plotted at the center of the p_T bin, and then corrected vertically by shifting it up or down. This is referred to as the up-down method.

To do the correction, we use the following formula (Eq 1 in AN 1001), which contains three parameters:

$$f(p_T) = p_0 \left(1 + \left(\frac{p_T}{p_1} \right)^2 \right)^{p_2} \quad (1)$$

The starting values for the three parameters p_1, p_2, p_3 were also taken from AN 1001 (Table I). For pp, the starting parameters listed are:

$$p_0 = 8.076 * 10^{-8} \quad p_1 = 3.68244 \quad p_2 = -5.72556 \quad (2)$$

For the North arm of Run08dAu:

$$p_0 = 3.9955 * 10^{-7} \quad p_1 = 3.7014 \quad p_2 = -5.37627 \quad (3)$$

And for the South arm of Run08dAu:

$$p_0 = 5.19894 * 10^{-7} \quad p_1 = 4.31213 \quad p_2 = -6.5886 \quad (4)$$

We applied these same parameters for Run08dAu to the Run15pAu, Run15pAl and Run14HeAu systems. The results of the binshift corrections for pp, pAu, pAl and HeAu are shown here.

In addition to these binshift corrections, there is also the set of binshift corrections for the corresponding pp invariant cross sections for pA, pAl and HeAu. If all four systems shared the same p_T binning, then only one set of binshift corrections for the pp invariant yield would be sufficient. But since we have used different p_T binning, we also need the correctly binned pp invariant cross section. A sample of these correction values are shown on page 11.

1.4 J/ψ Counts

The raw J/ψ counts are determined directly from the fitting function. The number of raw J/ψ counts are calculated by finding the area under the curve of the J/ψ peak. This is done by taking the integral of the J/Psi Crystal Ball function $f(x)$ over the x - axis invariant mass range extending from 2 - 5 GeV/c².

The y - axis units are J/ψ counts per invariant mass bin. The invariant mass binning used in this analysis is 50 MeV/c². Therefore, we have a dimensionless number of raw J/ψ counts. The results for all four small systems are shown in Tables 7 for the North arm and Table 8 for the South arm.

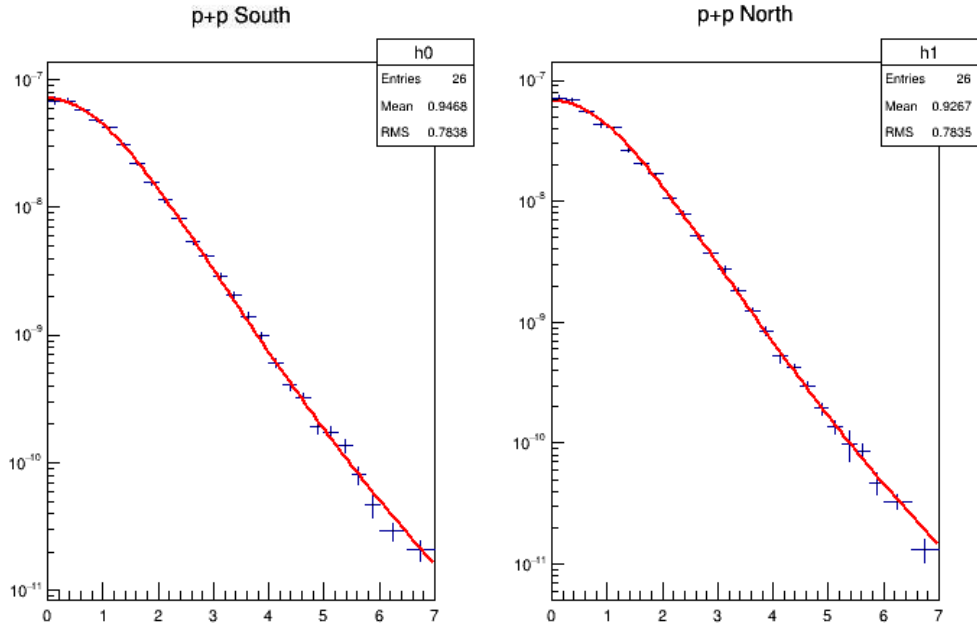


Figure 9: The bestfit function through the 26 data points of Run15pp, which are plotted along the (horizontal) center of the pt bins. If the data point is above the line of best fit, then the bin shift correction factor would be less than one. Similarly, if the data points falls below the line of bestfit, the correction factor would be greater than one.

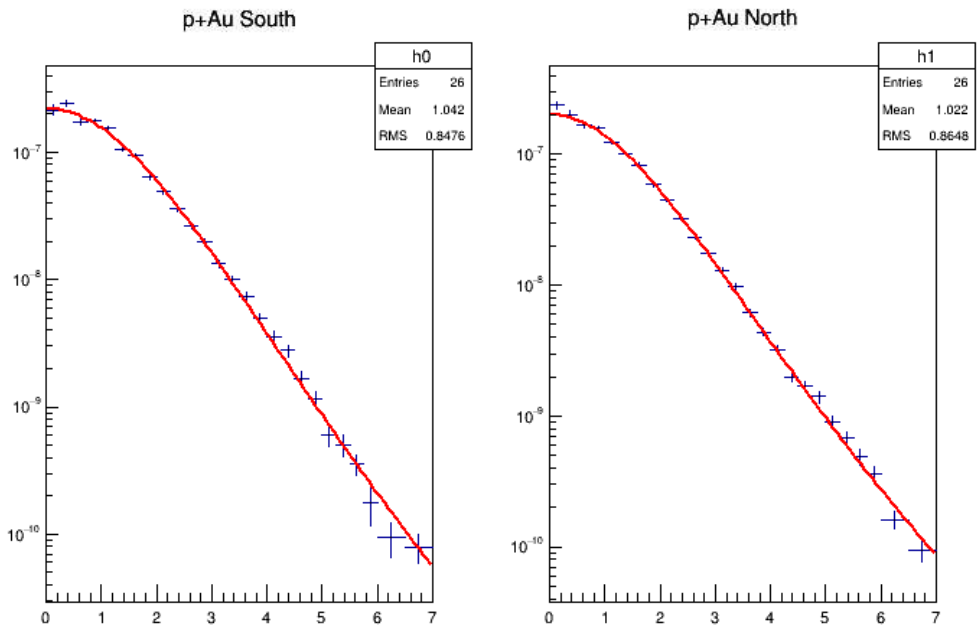


Figure 10: The bestfit function through the 26 data points of Run15pAu, which are plotted along the (horizontal) center of the pt bins.

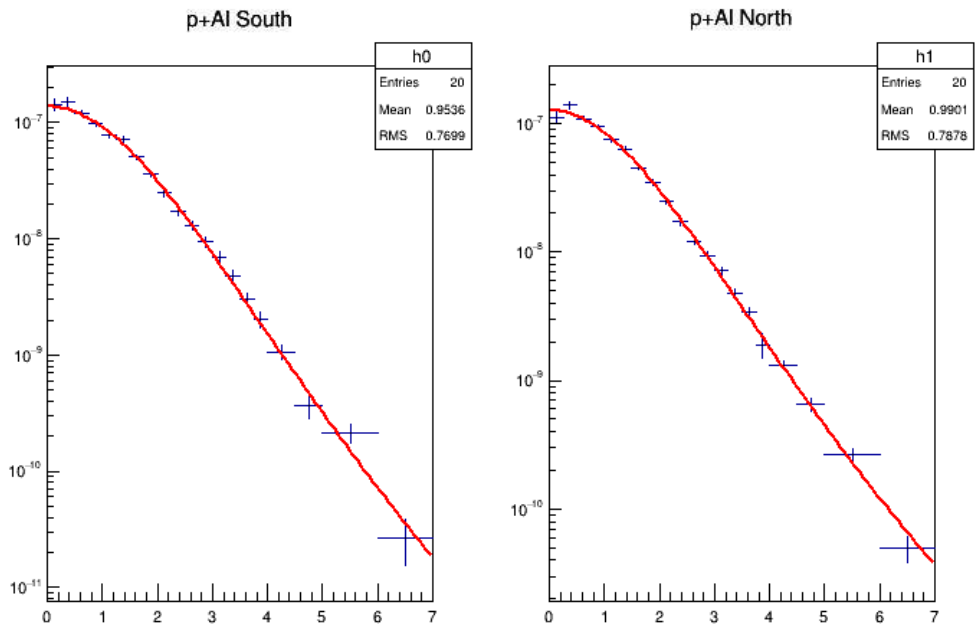


Figure 11: The bestfit function through the 20 data points of Run15pAl, which are plotted along the (horizontal) center of the pt bins.

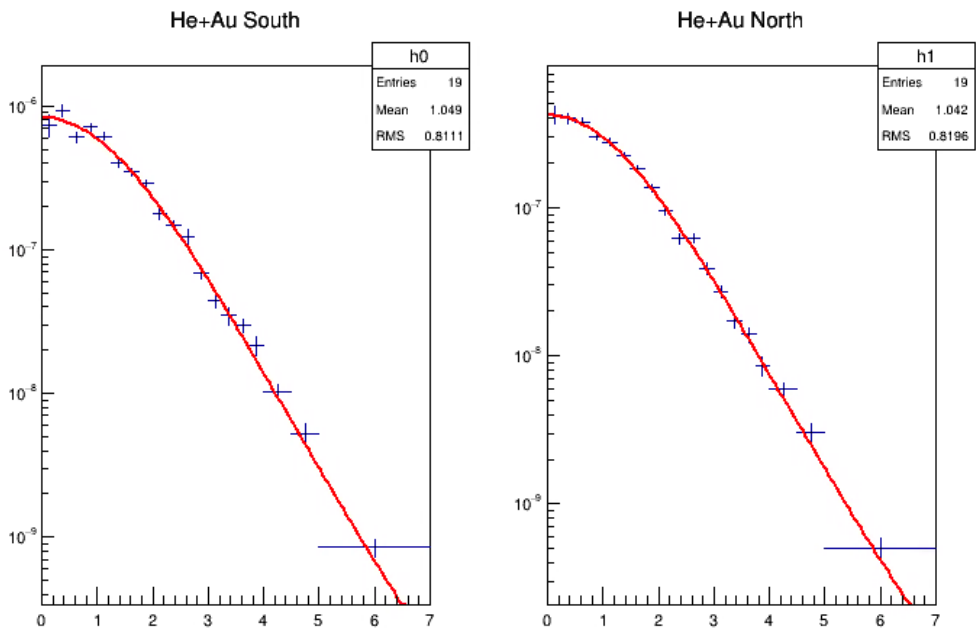


Figure 12: The bestfit function through the 19 data points of Run14HeAu, which are plotted along the (horizontal) center of the pt bins.

p+p North r = 0.997499, pt = 0.125
 p+p North r = 0.9979, pt = 0.375
 p+p North r = 0.998644, pt = 0.625
 p+p North r = 0.999631, pt = 0.875
 p+p North r = 1.00075, pt = 1.125
 p+p North r = 1.00187, pt = 1.375
 p+p North r = 1.00292, pt = 1.625
 p+p North r = 1.00384, pt = 1.875
 p+p North r = 1.00459, pt = 2.125
 p+p North r = 1.00516, pt = 2.375
 p+p North r = 1.00557, pt = 2.625
 p+p North r = 1.00583, pt = 2.875
 p+p North r = 1.00597, pt = 3.125
 p+p North r = 1.00601, pt = 3.375
 p+p North r = 1.00597, pt = 3.625
 p+p North r = 1.00587, pt = 3.875
 p+p North r = 1.00573, pt = 4.125
 p+p North r = 1.00556, pt = 4.375
 p+p North r = 1.00537, pt = 4.625
 p+p North r = 1.00516, pt = 4.875
 p+p North r = 1.00496, pt = 5.125
 p+p North r = 1.00475, pt = 5.375
 p+p North r = 1.00454, pt = 5.625
 p+p North r = 1.00433, pt = 5.875
 p+p North r = 1.01624, pt = 6.25
 p+p North_r = 1.01478, pt = 6.75

(a) *Run15pp North arm invariant yield bin shift correction value r , with the p_T value corresponding to the (horizontal) center of the bin*

p+p South r = 0.997512, pt = 0.125
 p+p South r = 0.997909, pt = 0.375
 p+p South r = 0.998647, pt = 0.625
 p+p South r = 0.999626, pt = 0.875
 p+p South r = 1.00073, pt = 1.125
 p+p South r = 1.00185, pt = 1.375
 p+p South r = 1.00288, pt = 1.625
 p+p South r = 1.00379, pt = 1.875
 p+p South r = 1.00453, pt = 2.125
 p+p South r = 1.00509, pt = 2.375
 p+p South r = 1.00549, pt = 2.625
 p+p South r = 1.00575, pt = 2.875
 p+p South r = 1.00589, pt = 3.125
 p+p South r = 1.00592, pt = 3.375
 p+p South r = 1.00588, pt = 3.625
 p+p South r = 1.00579, pt = 3.875
 p+p South r = 1.00564, pt = 4.125
 p+p South r = 1.00547, pt = 4.375
 p+p South r = 1.00528, pt = 4.625
 p+p South r = 1.00508, pt = 4.875
 p+p South r = 1.00488, pt = 5.125
 p+p South r = 1.00467, pt = 5.375
 p+p South r = 1.00446, pt = 5.625
 p+p South r = 1.00426, pt = 5.875
 p+p South r = 1.01597, pt = 6.25
 p+p South_r = 1.01453, pt = 6.75

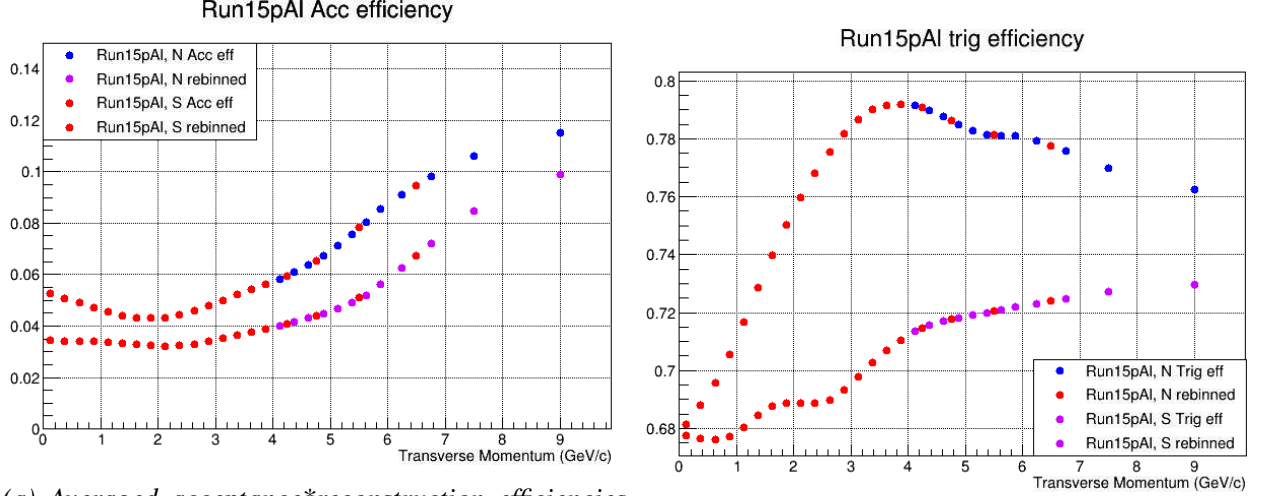
(b) *Run15pp South arm bin shift correction value r for each data point, with the p_T value corresponding to the (horizontal) center of the bin.*

Table 7: North arm raw J/ψ counts with statistical uncertainties obtained from the small systems study.

| p_T [GeV/c] | Run15pp, N | Run15pAu, N | Run15pAl, N | Run14HeAu, N |
|---------------------|--------------|--------------|--------------|--------------|
| 0.0 - 0.25 | 795 ± 35 | 420 ± 24 | 210 ± 19 | 75 ± 10 |
| 0.25 - 0.5 | 2147 ± 58 | 1063 ± 64 | 765 ± 52 | 211 ± 17 |
| 0.5 - 0.75 | 2737 ± 67 | 1428 ± 45 | 982 ± 41 | 328 ± 21 |
| 0.75 - 1.0 | 3413 ± 74 | 1870 ± 52 | 1155 ± 44 | 346 ± 21 |
| 1.0 - 1.25 | 3548 ± 77 | 1829 ± 52 | 1169 ± 60 | 405 ± 23 |
| 1.25 - 1.5 | 3045 ± 68 | 1815 ± 49 | 1180 ± 41 | 379 ± 22 |
| 1.5 - 1.75 | 2746 ± 64 | 1727 ± 50 | 981 ± 40 | 380 ± 23 |
| 1.75 - 2.0 | 2367 ± 61 | 1402 ± 47 | 869 ± 37 | 338 ± 21 |
| 2.0 - 2.25 | 1847 ± 53 | 1241 ± 40 | 715 ± 47 | 263 ± 18 |
| 2.25 - 2.5 | 1530 ± 66 | 1022 ± 37 | 566 ± 30 | 197 ± 19 |
| 2.5 - 2.75 | 1215 ± 57 | 861 ± 34 | 467 ± 28 | 226 ± 17 |
| 2.75 - 3.0 | 1043 ± 39 | 757 ± 31 | 419 ± 27 | 152 ± 14 |
| 3.0 - 3.25 | 838 ± 34 | 634 ± 36 | 366 ± 24 | 133 ± 13 |
| 3.25 - 3.5 | 675 ± 31 | 552 ± 26 | 275 ± 20 | 97 ± 11 |
| 3.5 - 3.75 | 493 ± 27 | 384 ± 22 | 221 ± 17 | 87 ± 10 |
| 3.75 - 4.0 | 354 ± 24 | 304 ± 20 | 134 ± 30 | 59 ± 8 |
| 4.0 - 4.25 | 247 ± 20 | 244 ± 18 | - | - |
| 4.25 - 4.5 | 212 ± 18 | 168 ± 14 | - | - |
| 4.0 - 4.5 | - | - | 218 ± 18 | 95 ± 11 |
| 4.5 - 4.75 | 170 ± 16 | 157 ± 15 | - | - |
| 4.75 - 5.0 | 118 ± 14 | 146 ± 15 | - | - |
| 4.5 - 5.0 | - | - | 132 ± 15 | 60 ± 9 |
| 5.0 - 5.25 | 103 ± 12 | 103 ± 12 | - | - |
| 5.25 - 5.5 | 83 ± 12 | 85 ± 10 | - | - |
| 5.5 - 5.75 | 68 ± 10 | 67 ± 9 | - | - |
| 5.75 - 6.0 | 38 ± 8 | 54 ± 8 | - | - |
| 5.0 - 6.0 | - | - | 143 ± 14 | - |
| 5.0 - 7.0 | - | - | - | 62 ± 10 |
| 6.0 - 6.5 | 64 ± 9 | 57 ± 8 | - | - |
| 6.5 - 7.0 | 27 ± 7 | 38 ± 7 | - | - |
| 6.0 - 7.0 | - | - | 39 ± 9 | - |
| Sum J/ψ counts | 29,960 | 18,456 | 11,028 | 3,895 |
| p_T integrated: | 29,597 ± 294 | 18,091 ± 244 | 11,158 ± 195 | 3,745 ± 103 |

Table 8: South arm raw J/ψ counts with statistical uncertainties obtained from the small systems study.

| p_T [GeV/c] | Run15pp, S | Run15pAu, S | Run15pAl, S | Run14HeAu, S |
|----------------------|--------------|--------------|-------------|--------------|
| 0.0 - 0.25 | 678 ± 32 | 216 ± 19 | 148 ± 16 | 69 ± |
| 0.25 - 0.5 | 1975 ± 57 | 727 ± 34 | 463 ± 42 | 264 ± |
| 0.5 - 0.75 | 2621 ± 65 | 876 ± 39 | 623 ± 35 | 289 ± |
| 0.75 - 1.0 | 3266 ± 73 | 1235 ± 45 | 714 ± 38 | 475 ± |
| 1.0 - 1.25 | 3446 ± 58 | 1400 ± 46 | 733 ± 35 | 519 ± |
| 1.25 - 1.5 | 3097 ± 66 | 1155 ± 41 | 815 ± 57 | 410 ± |
| 1.5 - 1.75 | 2708 ± 84 | 1184 ± 42 | 669 ± 35 | 413 ± |
| 1.75 - 2.0 | 2107 ± 56 | 927 ± 50 | 550 ± 33 | 390 ± |
| 2.0 - 2.25 | 1666 ± 53 | 806 ± 35 | 432 ± 35 | 270 ± |
| 2.25 - 2.5 | 1347 ± 45 | 661 ± 30 | 332 ± 27 | 254 ± |
| 2.5 - 2.75 | 1013 ± 39 | 545 ± 28 | 288 ± 22 | 240 ± |
| 2.75 - 3.0 | 905 ± 36 | 460 ± 26 | 235 ± 22 | 152 ± |
| 3.0 - 3.25 | 711 ± 31 | 354 ± 23 | 199 ± 19 | 111 ± |
| 3.25 - 3.5 | 536 ± 28 | 297 ± 20 | 153 ± 17 | 98 ± |
| 3.5 - 3.75 | 437 ± 26 | 247 ± 18 | 107 ± 14 | 93 ± |
| 3.75 - 4.0 | 334 ± 23 | 180 ± 16 | 79 ± 11 | 74 ± |
| 4.0 - 4.25 | 216 ± 18 | 142 ± 14 | - | - |
| 4.25 - 4.5 | 142 ± 16 | 122 ± 12 | - | - |
| 4.0 - 4.5 | - | - | 95 ± 13 | 81 ± 11 |
| 4.5 - 4.75 | 130 ± 15 | 82 ± 11 | - | ± |
| 4.75 - 5.0 | 84 ± 12 | 62 ± 10 | - | ± |
| 4.5 - 5.0 | - | - | 52 ± 9 | 50 ± 8 |
| 5.0 - 5.25 | 84 ± 12 | 36 ± 7 | - | - |
| 5.25 - 5.5 | 77 ± 10 | 34 ± 7 | - | - |
| 5.5 - 5.75 | 46 ± 9 | 26 ± 5 | - | - |
| 5.75 - 6.0 | 27 ± 7 | 15 ± 5 | - | - |
| 5.0 - 6.0 | - | - | 61 ± 11 | - |
| 5.0 - 7.0 | - | - | - | 55 ± 8 |
| 6.0 - 6.5 | 47 ± 15 | 19 ± 6 | - | - |
| 6.5 - 7.0 | 39 ± 8 | 20 ± 5 | - | - |
| 6.0 - 7.0 | - | - | 12 ± 5 | - |
| Sum J/ψ counts: | 27,764 | 11,855 | 6,770 | 4,300 |
| p_T integrated: | 28,288 ± 285 | 11,712 ± 256 | 6,660 ± 138 | 4,114 ± 99 |



1.5 Invariant Yield

The invariant yield, or the raw number of J/ψ counts which have been corrected for detector effects, was calculated using the following formula:

$$\frac{d^2 N}{dy dp_T} = \frac{cN}{2\pi p_T \epsilon \Delta y \Delta p_T N_{MB}}, \quad (5)$$

where c is the bias correction factor, N is the number of raw J/ψ counts for a particular fit, p_T is the corresponding center of the p_T bin used for the fit, ϵ is the product of trigger and acceptance efficiencies, Δy is the rapidity bin width used, Δp_T is the transverse momentum binwidth and N_{MB} is the number of minimum bias events for the subset of runs used.

Sanghoon Lim determined the acceptance reconstruction efficiencies as well as the trigger efficiencies. The binning used exactly matched Run15pp and Run15pAu, but in Run15pAl, the p_T bins above 4 GeV were rebinned by taking the mean of the efficiencies. The results of the averaged values are shown above.

All extracted J/ψ counts for the minimum bias study are listed in section 1.4. All extracted J/ψ counts for the centrality study are listed in section 2. The bias correction factors are listed in the following tables. The p_T bin widths used in this analysis are 0.25 GeV/c, 0.5 GeV/c, 1 GeV/c or 2 GeV/c. The bin width was increased at high p_T when J/ψ counts became too few to maintain good statistical certainty. We aimed for 50 or more J/ψ counts per bin for all small systems, as well as the centrality study for pAu. The rapidity bin width used is $1.2 < |y| < 2.2$. The number of uncorrected minimum bias events was determined by Sanghoon Lim, and are listed in the Tables 9, 10 (see AN1354).

Table 9: BBC and hard processes efficiencies followed by the (uncorrected) number of minimum bias events for North and South arms for the pp system.

| system | BBC efficiency | BBC efficiency for J/ψ events | Reference | N_{mb} North | N_{mb} South |
|----------|----------------|------------------------------------|-----------|-------------------|-------------------|
| Run15 pp | 0.55 | 0.79 | AN 1263 | $1.073 * 10^{12}$ | $1.092 * 10^{12}$ |

Table 10: Bias correction factors and N_{coll} followed by the (uncorrected) number of minimum bias events for North and South arms for the pAu, pAl and 3HeAu systems.

| system | N_{coll} | Bias correction factor | Reference | N_{mb} North | N_{mb} South |
|-------------|------------|------------------------|-----------|-------------------|-------------------|
| Run15 pAu | 4.667 | 0.858 | AN 1265 | $1.936 * 10^{11}$ | $2.103 * 10^{11}$ |
| Run15 pAl | 2.10 | 0.80 | AN 1290 | $2.007 * 10^{11}$ | $2.042 * 10^{11}$ |
| Run14 3HeAu | 10.4 | 0.89 | AN 1207 | | |

1.5.1 Invariant Yield Results

We plotted the invariant yields for both the North and South arms in all four systems. These plots are shown in Figures 15, 16.

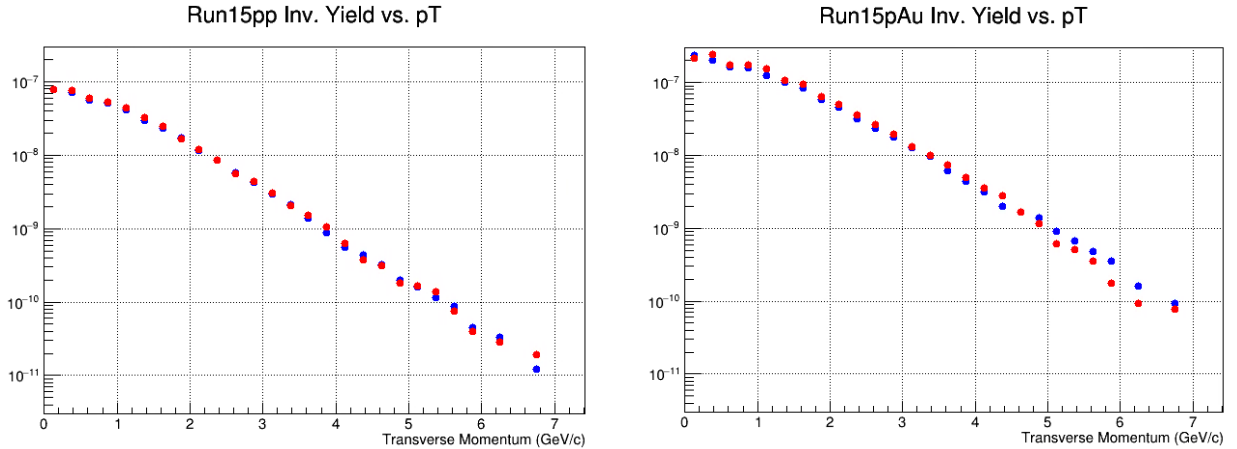


Figure 15: Run15pp (left) and Run15pAu Invariant yield results as a function of p_T .

1.6 Invariant Cross Section

The invariant cross section is found by simply multiplying the Invariant yield by the (uncorrected) BBC cross section for sqrt(200) GeV p+p, which is 42 mb. NOTE: For Run14HeAu, N_{coll} is currently estimated, and the trigger and acceptance efficiencies are borrowed from Run15pAu. Additionally, the systematic trigger uncertainties are from Run15pp.

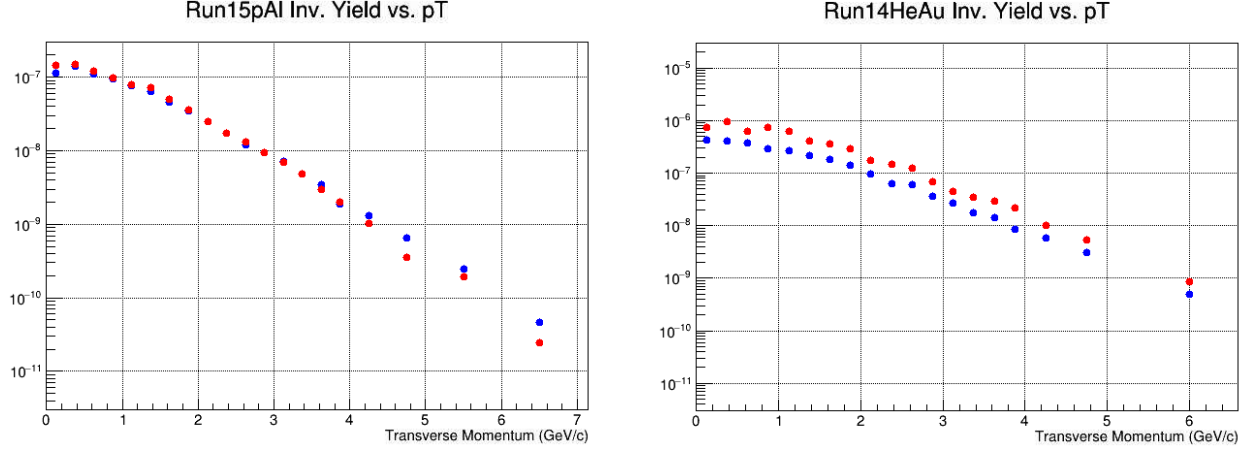


Figure 16: Run15pAl (left) and Run14HeAu Invariant yield results as a function of p_T . NOTE: N_{MB} is currently a guessed figure in Run14HeAu, and trigger and acceptance efficiencies in Run14HeAu are taken from Run15pAu.

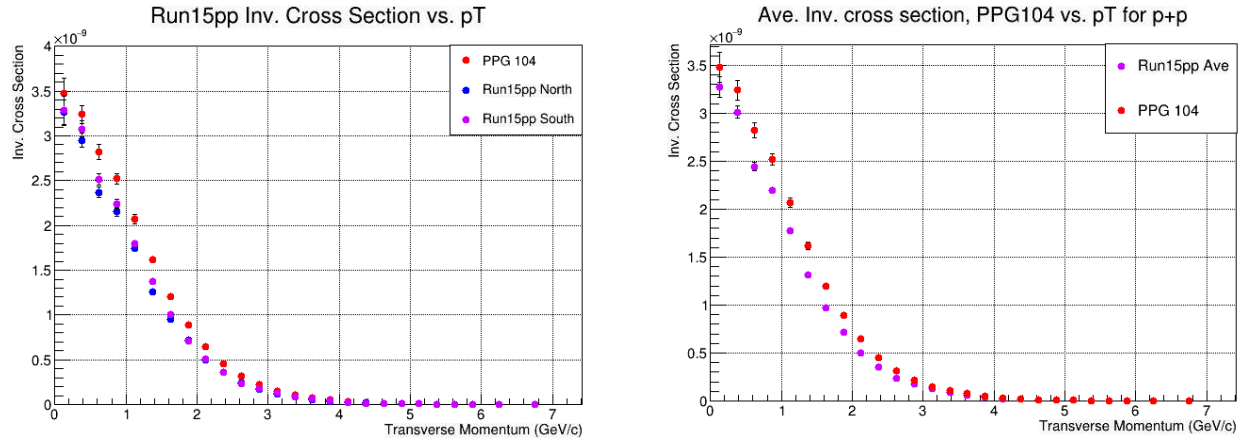


Figure 17: Run15 pp results. Left: Invariant cross sections, compared with PPG 104 results. Right: PPG104 compared with the average value of Run15pp.

1.7 R_{AA} vs. p_T

1.7.1 Run15pAu, Run15pAl and Run14HeAu Results

We have extracted the J/ψ raw counts from the data, and listed the results in Tables 7, 8. Here we have determined R_{pAu} for the North and South arm, and compared it with the results from PPG 125. The error bars are Type A uncertainties (uncorrelated point to point) while the boxes are Type B uncertainties (correlated point to point). The Type A uncertainties are the uncertainties in the counts of Tables 7, 8. The Type B and C uncertainties are listed in Tables 11, 12.

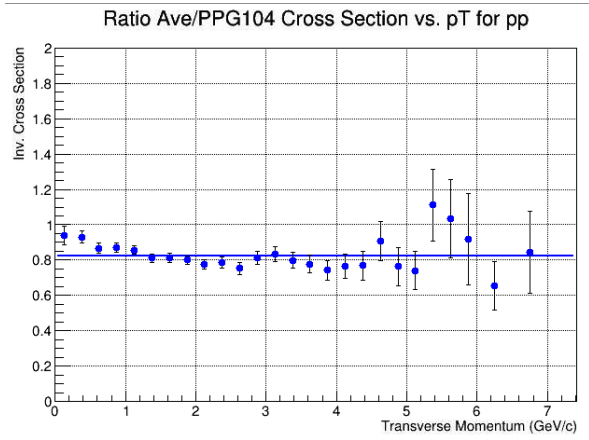
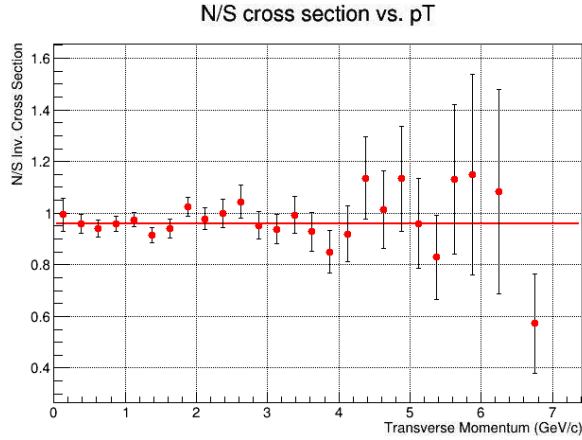


Figure 18: Run15pp results. Left: The ratio of North arm to South arm. Right: The ratio of the average compared with PPG104.

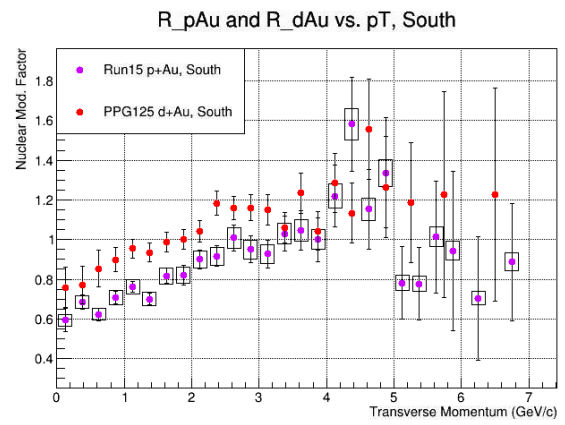
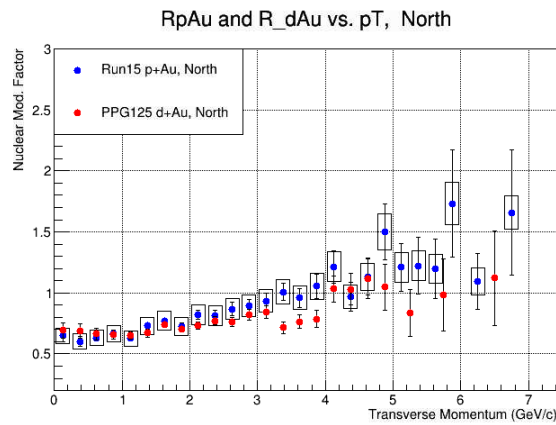


Figure 19: Run15pAu R_{pAu} compared with PPG125 R_{dAu} in the North, left, and South.

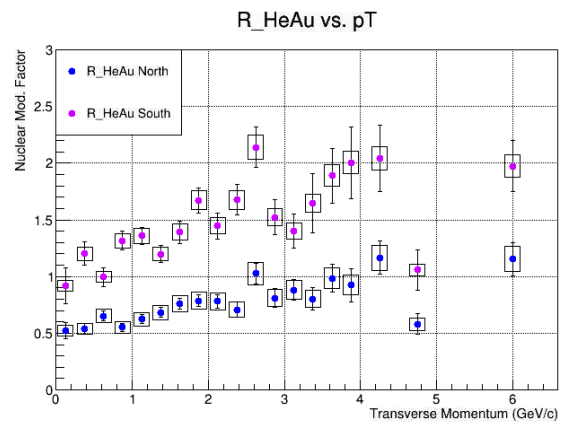
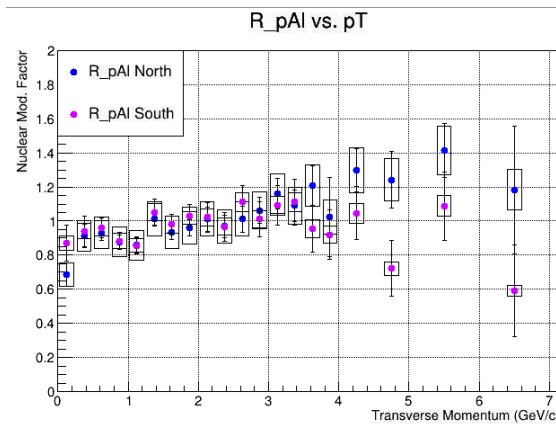
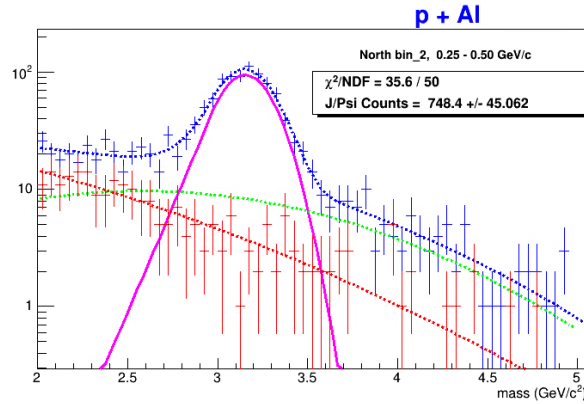


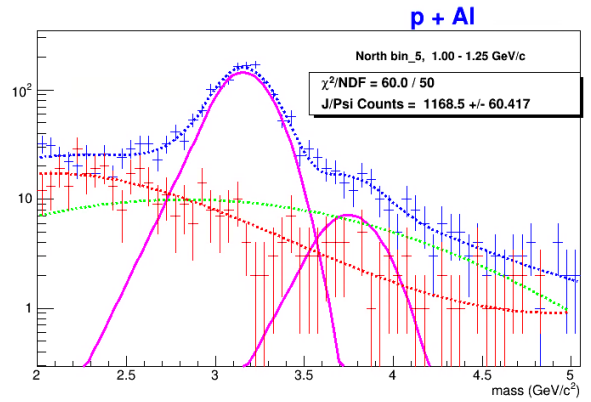
Figure 20: Left: Run15pAl R_{pAu} results. Right: Run14HeAu R_{pAu} results. NOTE: Run14HeAu analysis is currently using a guessed figure for N_{MB} , Run15pAu trigger and acceptance efficiencies, and systematic trigger uncertainties taken from Run15pp.

1.8 Example Fits

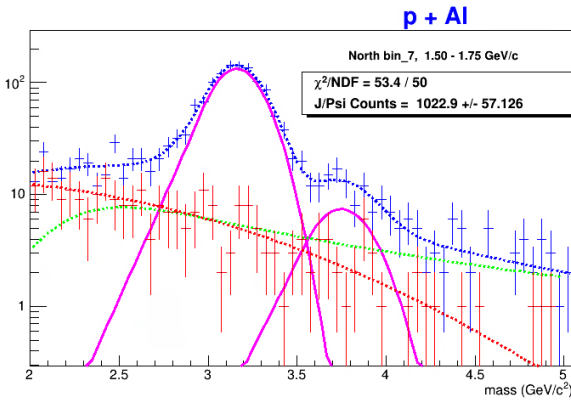
1.8.1 Test fits from Run15pAl



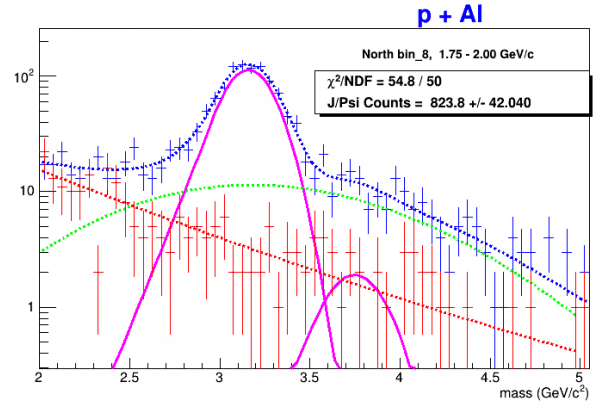
(a) Run15pAl North arm test fit 1/5. All test fits had to fit a set of criteria (see section 2.2)



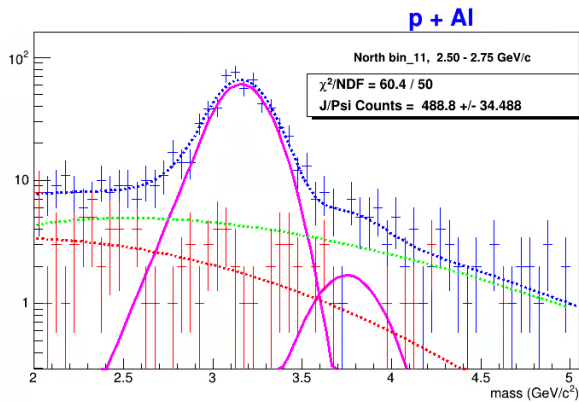
(b) Run15pAl North arm test fit 2/5.



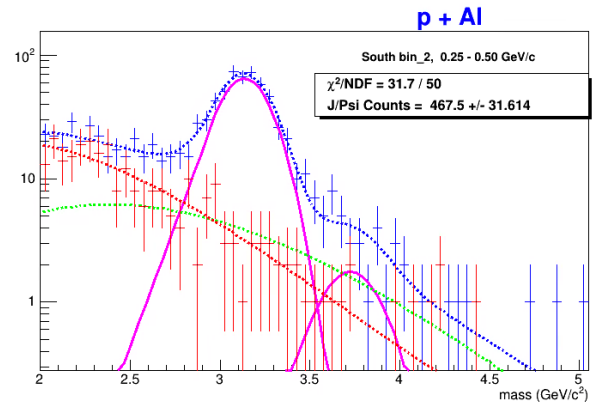
(a) Run15pAl North arm test fit 3/5.



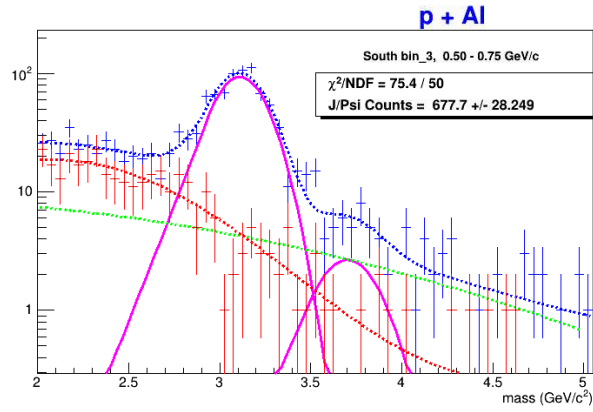
(b) Run15pAl North arm test fit 4/5.



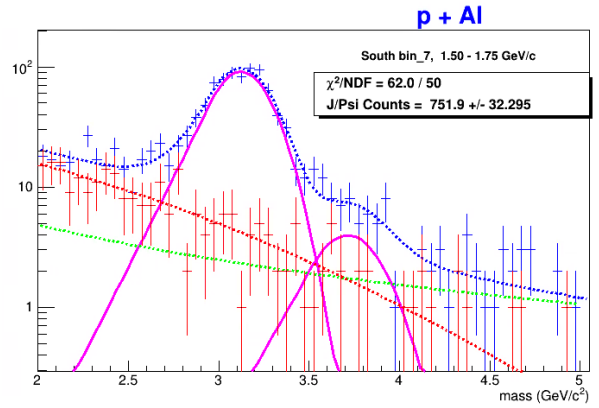
(a) Run15pAl North arm test fit 5/5.



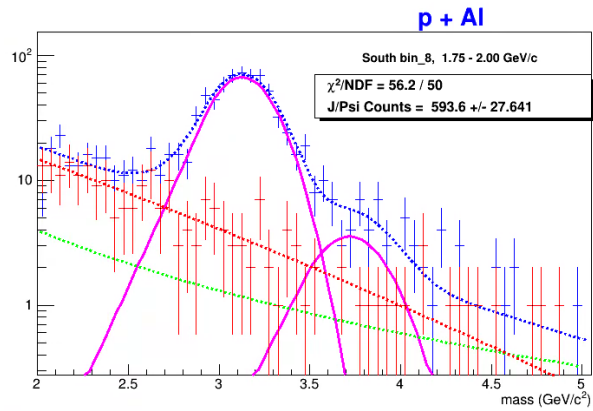
(b) Run15pAl South arm test fit 1/5.



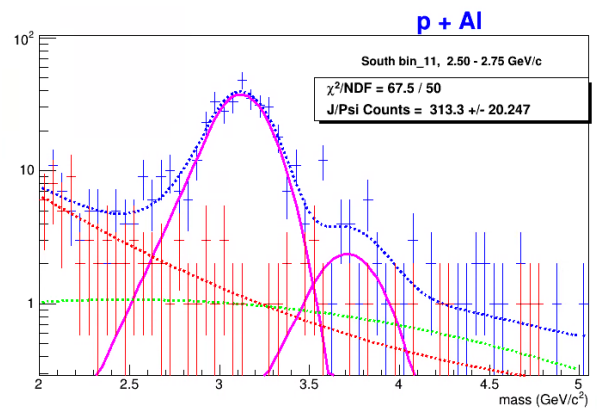
(a) Run15pAl South arm test fit 2/5.



(b) Run15pAl South arm test fit 3/5.

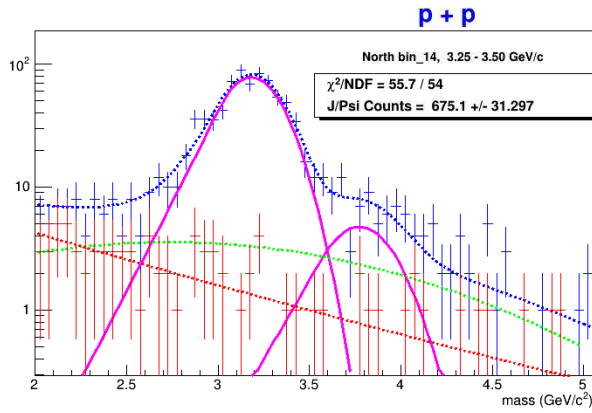


(a) Run15pAl South arm test fit 4/5.

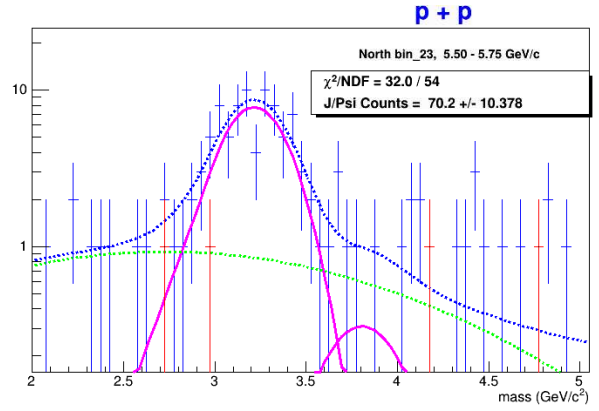


(b) Run15pAl South arm test fit 5/5.

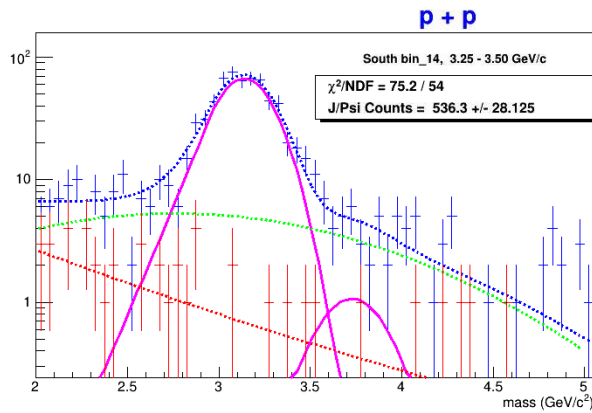
1.8.2 Sample Fits Using Fixed Correlated Background Parameters



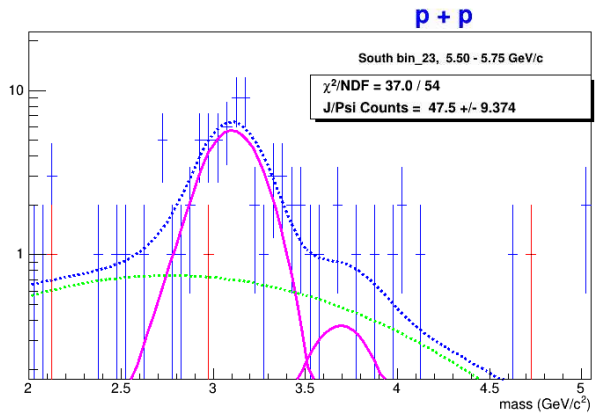
(a) Run15pp North arm example fit with fixed correlated background parameters.



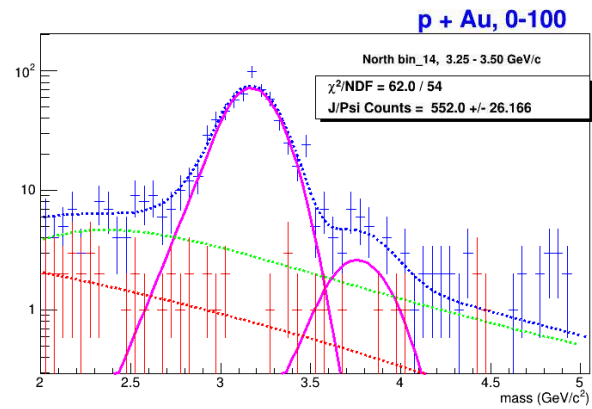
(b) Run15pp North arm fit with the same fixed correlated background parameters shown at left.



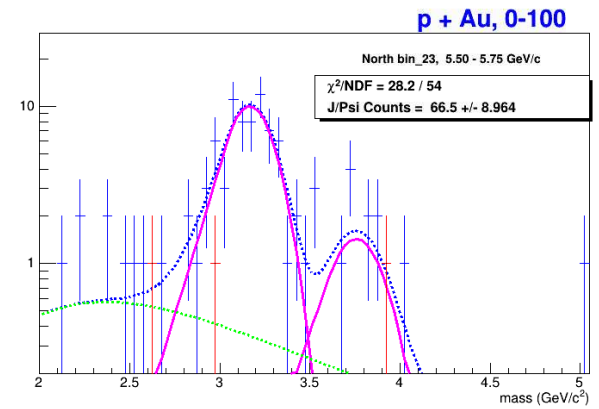
(a) Run15pp South arm example fit with fixed correlated background parameters.



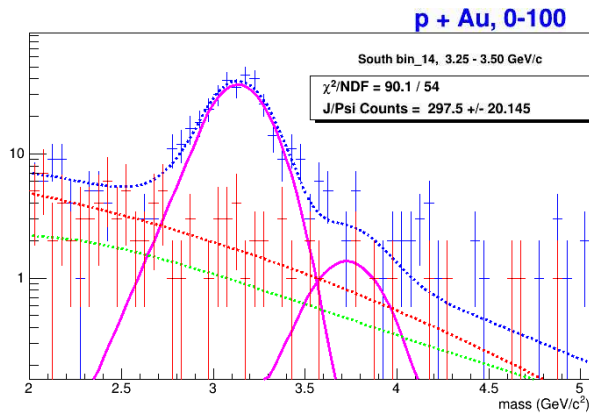
(b) Run15pp South arm fit with the same fixed correlated background parameters shown at left.



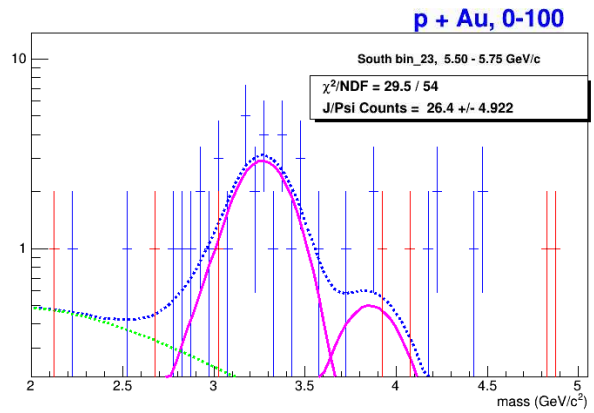
(a) Run15pAu North arm example fit with fixed correlated background parameters.



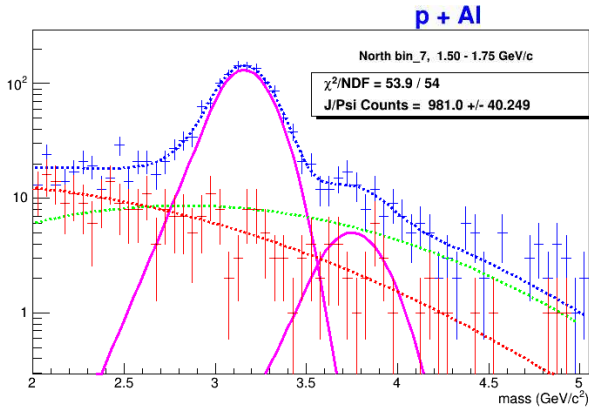
(b) Run15pAu North arm fit with the same fixed correlated background parameters shown at left.



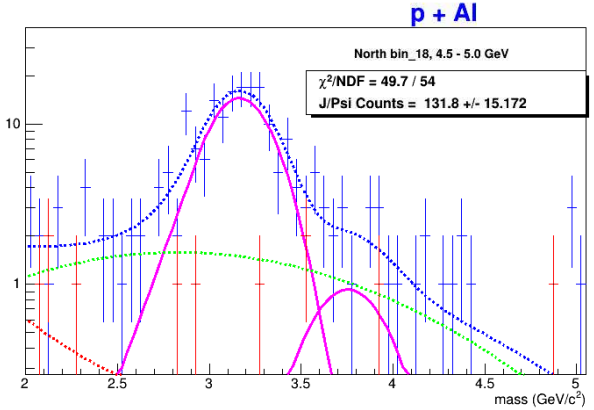
(a) Run15pAu South arm example fit with fixed correlated background parameters.



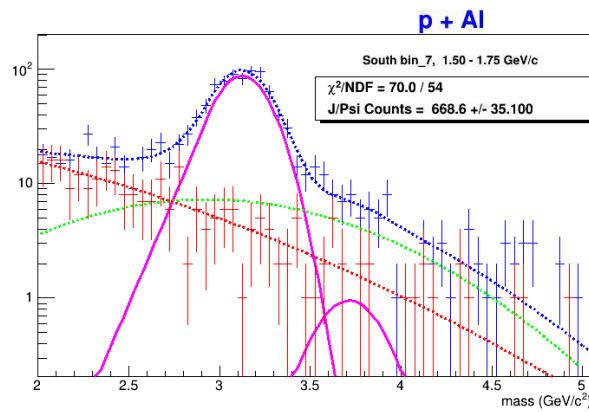
(b) Run15pAu South arm fit with the same fixed correlated background parameters shown at left.



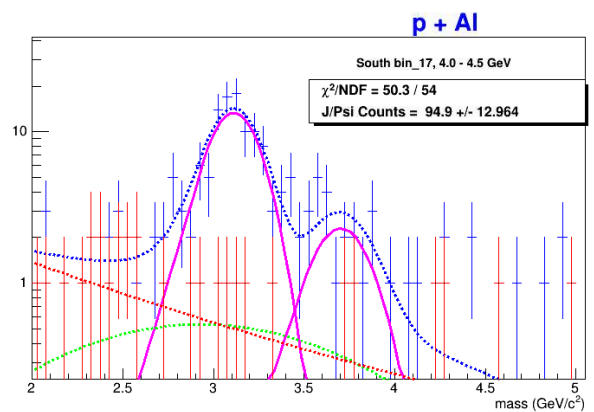
(a) Run15pAl North arm example fit with fixed correlated background parameters.



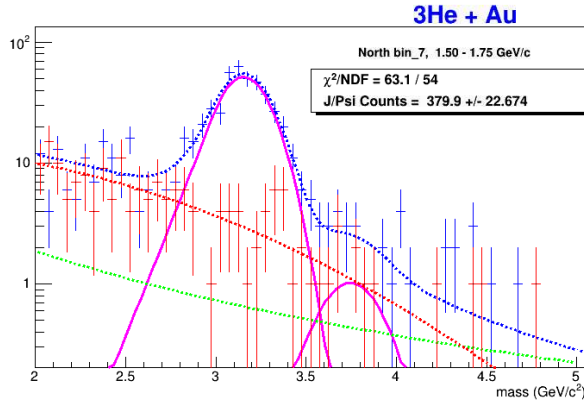
(b) Run15pAl North arm fit with the same fixed correlated background parameters shown at left.



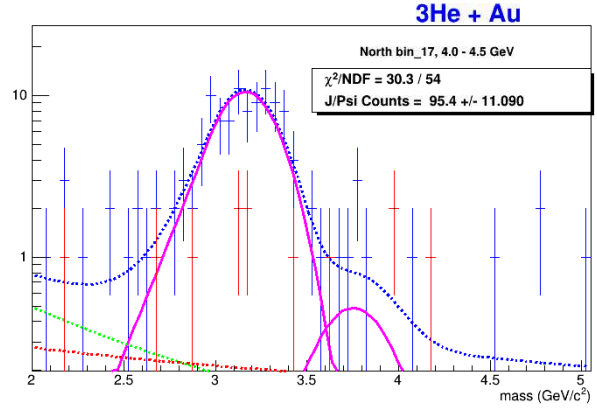
(a) Run15pAl South arm example fit with fixed correlated background parameters.



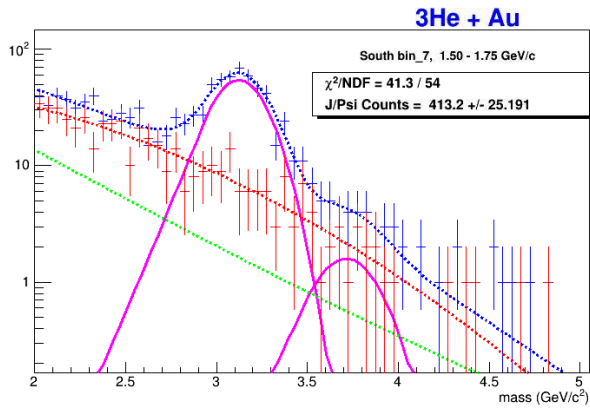
(b) Run15pAl South arm fit with the same fixed correlated background parameters shown at left.



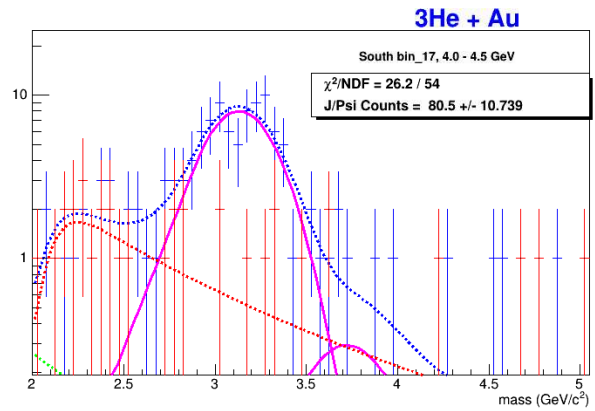
(a) Run14HeAu North arm example fit with fixed correlated background parameters.



(b) Run14HeAu North arm fit with the same fixed correlated background parameters shown at left.



(a) Run14HeAu South arm example fit with with fixed correlated background parameters.



(b) Run14HeAu South arm fit with the same fixed correlated background parameters shown at left.

1.9 Systematic Uncertainty

Here we list the systematic uncertainties in this analysis, as Type B or Type C. These include the uncertainties arising from: the correlated background shape, run to run variations, matching MuTr ϕ acceptance, initial distribution shape, 2D trigger efficiency, BBC bias correction factor, N_{coll} and a global BBC uncertainty.

Table 11: Type B systematic uncertainties for the North and South arms in all systems.

| System | Corr. bg | Run to Run Var. | MuTR ϕ Matching | Initial Shape | Trigger eff. |
|-------------|----------|-----------------|----------------------|---------------|--------------|
| Run15pp N | 0.0331 | 0.040 | 0.058 | 0.02 | 1.0 - 5.4% |
| Run15pp S | 0.0248 | 0.047 | 0.050 | 0.02 | 1.0 - 7.3% |
| Run15pAu N | 0.0363 | 0.016 | 0.034 | 0.02 | 1.0 - 5.4% |
| Run15pAu S | 0.0163 | 0.035 | 0.040 | 0.02 | 1.0 - 8.7% |
| Run15pAl N | 0.0359 | 0.028 | 0.036 | 0.02 | 1.0 - 1.8% |
| Run15pAl S | 0.0264 | 0.033 | 0.033 | 0.02 | 2.0 - 4.6% |
| Run14HeAu N | 0.0173 | 0.015 | 0.031 | 0.02 | 1.0 - 4.6% |
| Run14HeAu S | 0.0148 | 0.050 | 0.025 | 0.02 | 1.0 - 5.0% |

Table 12: Type C systematic uncertainties for the North and South arms in all systems.

| System | N_{coll} | bias correction factor | Reference | BBC |
|---------------|------------|------------------------|-----------|-----|
| Run15pp N/S | - | - | - | 10% |
| Run15pAu N/S | 0.3 | 0.014 | AN1265 | 10% |
| Run15pAl N/S | 0.1 | 0.02 | AN1290 | 10% |
| Run14HeAu N/S | 0.7 | 0.01 | AN1207 | 10% |

Of the five systematic uncertainties listed here, only the trigger efficiency is p_T dependent. We did not list each uncertainty, but rather reported the systematic as a range of uncertainties. In the case of R_{AA} , the MuTr efficiencies cancel. Otherwise, all listed uncertainties are included in the systematic errors, represented as boxes enclosing the data points. The run to run variation uncertainties were reported in AN1354 (section 5.2). The MuTr ϕ matching was also reported in AN1354, section 5.3. The trigger efficiencies for Run15pAu and Run14HeAu were reported in AN1354 section 5.5 as well. Since all uncertainties listed are in the form of fractional uncertainties, they can be added in quadrature (the square root of the sum of the squares). Type C uncertainties, which are uncorrelated systematic uncertainties, are listed in Table 12.

2 J/ψ as function of Centrality

2.1 Fitting

We analyzed the centrality dependence of the J/ψ in Run15pAu and Run15pAl systems over the following centrality ranges: 0 – 20, 20 – 40, 40 – 60, and 60 – 84. To make the fitting easier, we fixed four of the five correlated background parameters, and determined the overall systematic uncertainty using the methods described in the following sections.

We sampled five different test fits for each centrality range, and then applied the bestfit correlated background parameters to the other four fits, obtaining a total of 25 fits. We then selected the fit with the least spread as the best set of correlated background parameters, and used that set to fit all p_T bins in the centrality range.

2.2 Fixing the Correlated Background Parameters

To fix the background parameters, we took 5 very good "test" fits from each centrality range, at a different p_T value. Test fits were considered if they had less than 10 percent statistical uncertainty, a χ^2/NDF less than 1.5, looked visually reasonable, at least 130 J/ψ counts and also had well defined background parameters (meaning at least four out of the five parameters had errors smaller than the listed value, and the fifth error was on the order of the listed value).

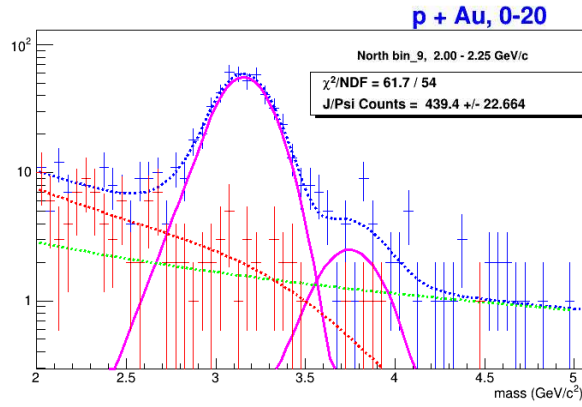
The bestfit values for the five parameters were recorded for each of the five fits. Then the bestfit parameters were applied to each of the other four fits. Therefore, one p_T data set was fitted five times, using the bestfit parameters of the 5 test fits. We also took 5 test fits for the minimum bias on each arm. It was determined that all fits converged.

The test fit that was determined as the bestfit is shown in figure [], for either the north or south arm. We have also included the test fit applied to a different p_T bin in the same centrality range. Examples are shown for each centrality range as well as the integrated p_T .

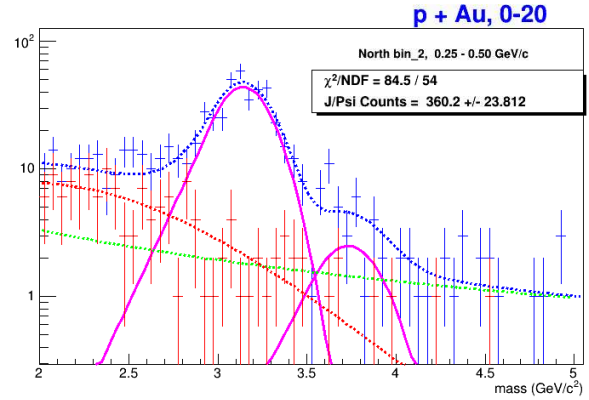
2.3 Systematic Uncertainty due to Correlated Background

The average number of J/ψ counts was calculated, from which then the RMS value was determined. The RMS value was then scaled by the mean J/ψ counts. Then for each centrality bin, we had a total of five scaled RMS values. We selected the smallest scaled RMS value as the test fit with the best set of correlated background parameters. This set of parameters was then used to fit all p_T bins for that particular centrality range.

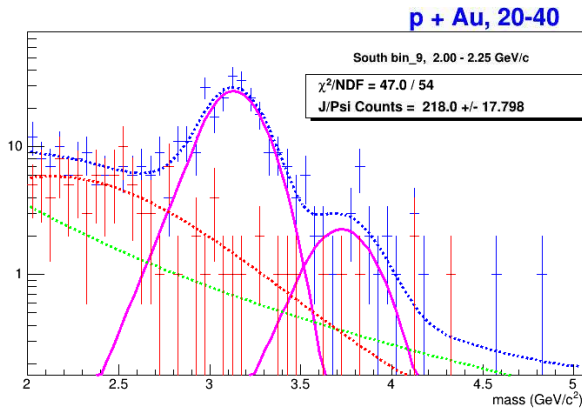
These 5 uncertainties were plotted for each centrality bin. As an example, see the 0 – 20% centrality range for the south arm in figure []. From these plots, it was determined that the overall systematic uncertainty for each centrality range was simply the average of the 5 uncertainties. The uncertainties for each fit in each centrality range are listed in table [].



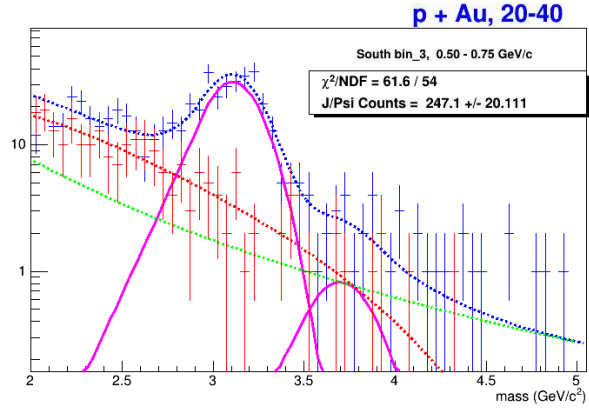
(a) Centrality 0 – 20%: The best "test" fit selected in the North arm (corresponds to data in the p_T range 2.0 – 2.25 GeV/c). This set of correlated background parameters was determined to have the least spread in J/ψ counts, and was used to fit all other data in the centrality range.



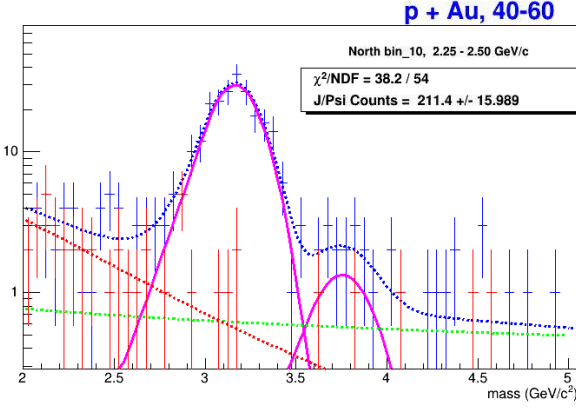
(b) Example: The correlated background parameters of the test fit shown on the left applied to the p_T range 0.25 – 0.50 GeV/c.



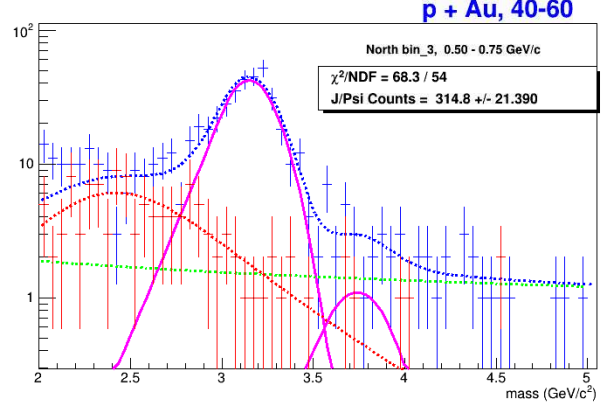
(a) Centrality 20 – 40%: The best "test" fit selected in the South arm (corresponds to data in the p_T range 2.0 – 2.25 GeV/c).



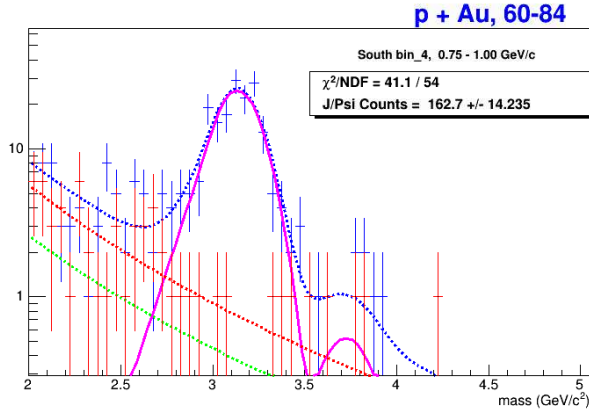
(b) Example: The correlated background parameters of the test fit shown on the left applied to the p_T range 0.50 – 0.75 GeV/c.



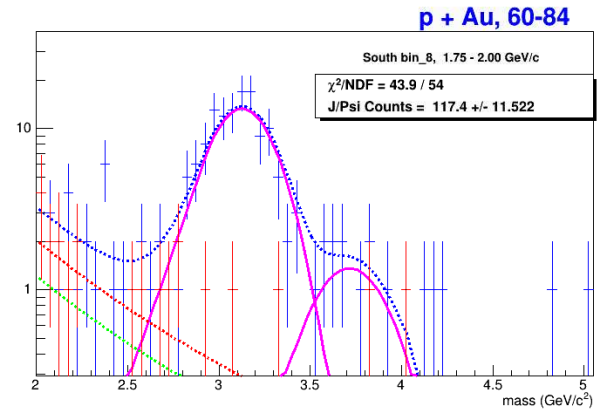
(a) Centrality 40 – 60%: The best "test" fit selected in the North arm (corresponds to data in the p_T range 2.25 – 2.50 GeV/c).



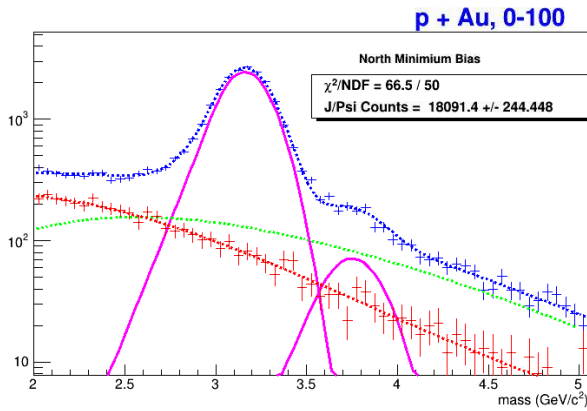
(b) Example: The correlated background parameters of the test fit shown on the left applied to the p_T range 0.50 – 0.75 GeV/c.



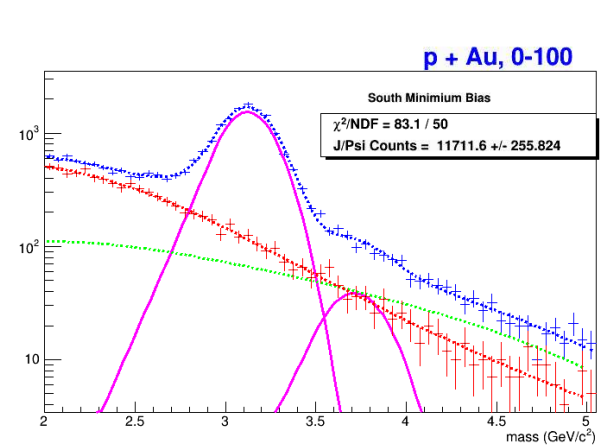
(a) Centrality 60 – 84%: The best "test" fit selected in the South arm (corresponds to data in the p_T range 0.75 – 1.0 GeV/c).



(b) Example: The correlated background parameters of the test fit shown on the left applied to the p_T range 1.75 – 2.0 GeV/c.



(a) Integrated p_T , North arm: The fit selected gave the best agreement with AN1354 results (see section 1.1.1).



(b) Integrated p_T , South arm: The fit selected gave the best agreement with AN1354 results.

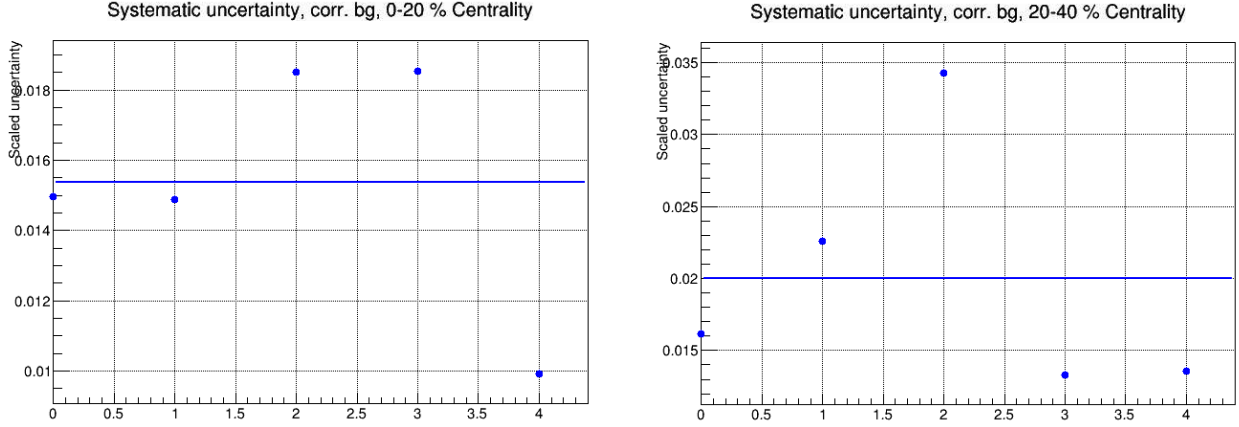


Figure 39: The scaled systematic uncertainties arising in the North arm from correlated background parameters plotted for each of the five fits for centrality range 0 – 20%, left and 20 – 40%, right. The line of best fit is the average.

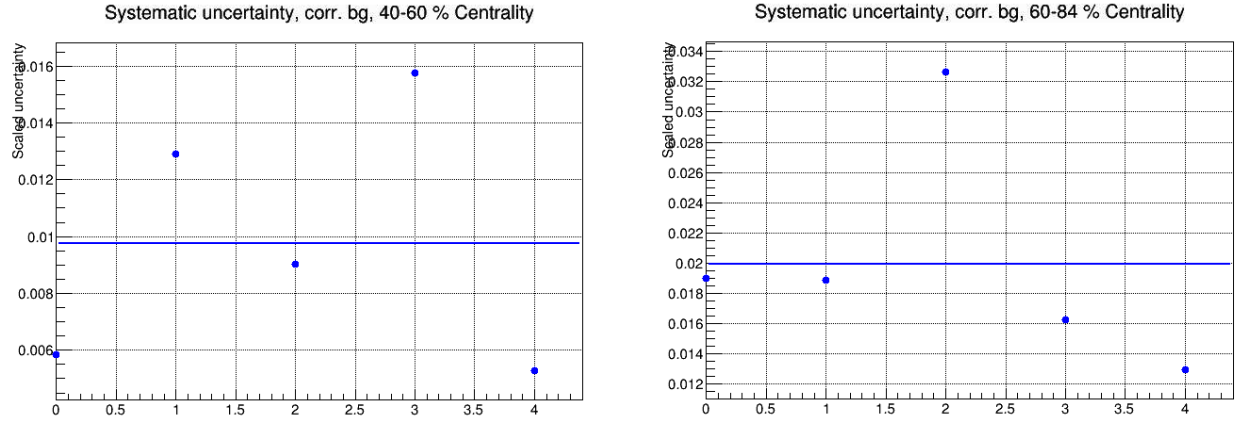


Figure 40: The scaled systematic uncertainties arising in the North arm from correlated background parameters plotted for each of the five fits for centrality range 40 – 60%, left and 60 – 84%, right. The line of best fit is the average.

To find the overall systematic uncertainty in each arm, we plotted the averaged uncertainty for each centrality bin. These uncertainties are shown as the first 4 data points in the figure [].

For the minimum bias, the same method was applied. The J/ψ counts were averaged, and again, an RMS value could be calculated. It was also scaled by the mean J/ψ counts, and this is shown as the fifth data point in the figure.

Based on the results of these five data points, the line of best fit is again the average of the five points, one averaged uncertainty for the north arm and another for the south. We have therefore assigned an overall systematic uncertainty for the correlated background as the average of all 4 uncertainties in the centrality ranges plus the uncertainty from the minimum bias. This result is listed in Table 13.

Table 13: Scaled uncertainties for each sampled "test" fit, the test fit p_T bin and the corresponding average for each centrality range.

| Centrality | p_T [GeV/c] | Scaled Uncertainty, N | p_T [GeV/c] | Scaled Uncertainty, S |
|------------|--------------------------|-------------------------|--------------------------|-------------------------|
| 0 – 20% | 0.75 – 1.00 | 0.0150 | 0.75 – 1.00 | 0.0098 |
| 0 – 20% | 1.00 – 1.25 | 0.0149 | 1.00 – 1.25 | 0.0089 |
| 0 – 20% | 1.25 – 1.50 | 0.0185 | 1.25 – 1.50 | 0.0412 |
| 0 – 20% | 1.75 – 2.00 | 0.0185 | 1.75 – 2.00 | 0.0195 |
| 0 – 20% | 2.00 – 2.25 | 0.0099 | 2.00 – 2.25 | 0.0089 |
| | Ave. Uncertainty: | 0.0154 | Ave. Uncertainty: | 0.0177 |
| 20 – 40% | 0.25 – 0.5 | 0.0161 | 0.50 – 0.75 | 0.0427 |
| 20 – 40% | 1.25 – 1.50 | 0.0226 | 0.75 – 1.00 | 0.0317 |
| 20 – 40% | 1.50 – 1.75 | 0.0343 | 1.25 – 1.50 | 0.0303 |
| 20 – 40% | 2.00 – 2.25 | 0.0133 | 1.50 – 1.75 | 0.0421 |
| 20 – 40% | 2.25 – 2.50 | 0.0136 | 2.00 – 2.25 | 0.0293 |
| | Average: | 0.0200 | Average: | 0.0352 |
| 40 – 60% | 0.25 – 0.50 | 0.0058 | 0.75 – 1.00 | 0.0086 |
| 40 – 60% | 0.50 – 0.75 | 0.0129 | 1.00 – 1.25 | 0.0102 |
| 40 – 60% | 1.00 – 1.25 | 0.0090 | 1.25 – 1.50 | 0.0060 |
| 40 – 60% | 1.75 – 2.00 | 0.0158 | 1.50 – 1.75 | 0.0093 |
| 40 – 60% | 2.25 – 2.50 | 0.0053 | 1.75 – 2.00 | 0.0090 |
| | Average: | 0.0098 | Average: | 0.0086 |
| 60 – 84% | 0.50 – 0.75 | 0.0190 | 0.75 – 1.00 | 0.0322 |
| 60 – 84% | 1.00 – 1.25 | 0.0188 | 1.00 – 1.25 | 0.0461 |
| 60 – 84% | 1.25 – 1.50 | 0.0327 | 1.25 – 1.50 | 0.0701 |
| 60 – 84% | 1.50 – 1.75 | 0.0162 | 1.50 – 1.75 | 0.0401 |
| 60 – 84% | 1.75 – 2.00 | 0.0130 | 1.75 – 2.00 | 0.0524 |
| | Average: | 0.0199 | Average: | 0.0482 |

Table 14: Run15pAu bias correction factors and N_{coll} for different centrality ranges. Reference: AN 1265.

| Centrality | N_{coll} | Bias correction factor |
|------------|---------------|------------------------|
| 0 – 20% | 8.8 ± 0.5 | 0.90 ± 0.01 |
| 20 – 40% | 6.1 ± 0.4 | 0.98 ± 0.01 |
| 40 – 60% | 4.4 ± 0.3 | 1.02 ± 0.01 |
| 60 – 84% | 2.6 ± 0.2 | 1.00 ± 0.06 |

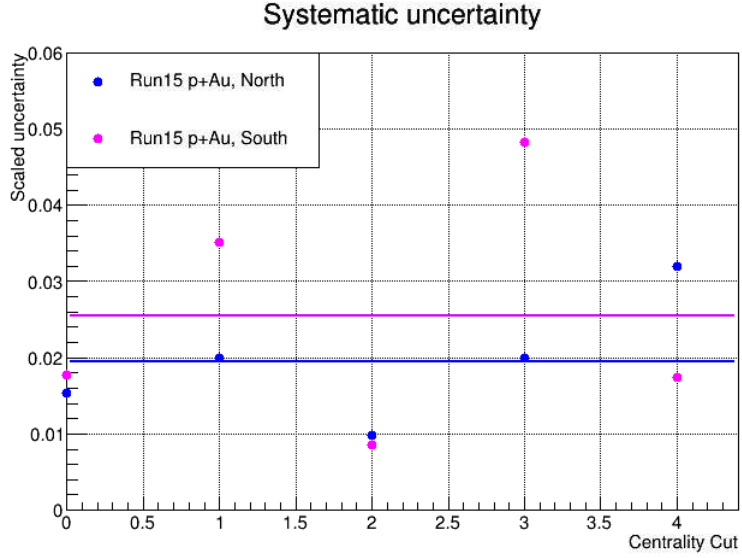


Figure 41: Averaged systematic uncertainties arising from correlated background parameters plotted for each centrality range (in sequential order). The last data point is the systematic uncertainty calculated for the minimum bias.

2.4 J/ψ Counts

2.5 R_{AA} as function of Centrality

2.5.1 Run15pAu Results